Star Formation Newsletter No. 338, #1-7

#1 A Theoretical Framework for the Mass Distribution of Gas Giant Planets Forming through the Core Accretion Paradigm, F. Adams et al., ApJ, 909,1
#2 Particle Dynamics in 3D Self-gravitating Disks. I. Spirals, H. Baehr & Z. Zhu, ApJ, 909, 135
#3 Particle Dynamics in 3D Self-gravitating Disks. II. Strong Gas Accretion and Thin Dust Disks, ApJ, 909, 136
#4 A possible far-ultraviolet flux-dependent core mass function in NGC 6357, J. Brand et al., A&A
#5 Tracers of the ionization fraction in dense and translucent gas: I. Automated exploitation of massive astrochemical model grids, E. Bron et al. A&A, 645, A28 (open access)
#6 Radial Velocity Monitoring of the Young Star Hubble 4: Disentangling Starspot Lifetimes from Orbital Motion, A. Carvalho et al. ApJ?
#7 The Extraordinary Outburst in the Massive Protostellar System NGC 6334 I-MM1: Spatiokinematics of Water Masers during a Contemporaneous Flare Event, ApJ, 908, 175

花輪 知幸

#1 A Theoretical Framework for the Mass Distribution of Gas Giant Planets Forming through the Core Accretion Paradigm, F. Adams et al., ApJ, 909,1

円盤は指数関数的に減少するのに、巨大ガス惑星の質量分布が

$\propto M_{\rm P}^{-p}$となるのはなぜ？

Core accretion paradigm

Phase I　コアの形成　(微惑星の衝突など)

Phase II　ゆっくりした降着による成長

Phase III　急速な降着による成長

$$M_{\rm p} = M_{\rm II} + \int_{t_{\rm onset}}^{t_{\rm end}} \dot{M}_{\rm p}(t)\,dt = M_{\rm II} + \langle \dot{M}_{\rm p} \rangle (t_{\rm end} - t_{\rm onset}), \quad (1)$$

観測と整合的なモデルをつくる

円盤を持つ割合

$$\frac{dF}{dt} = \frac{1}{\tau}\exp(-t/\tau),$$

τ = 4-5 Myr

mass distribution has an approximately power-law form over the mass range of interest $0.1M_{\rm J} \leqslant M_{\rm p} \leqslant 10M_{\rm J}$, i.e.,

$$\frac{dF}{dM_{\rm p}} = \frac{A}{M_{\rm p}^{p}} \qquad \text{where} \qquad p \approx 1.3 \pm 0.2, \qquad (2)$$

$$\dot{M}_{\rm d} = \dot{M}_{d(0)} \frac{m^2}{(1 + t/t_0)^{3/2}},$$

$t_0 \sim 1$Myr

$$t_{\rm onset} = t_{\rm c0}\, m^{1/2}, \qquad (8)$$

where we expect that $t_{\rm c0} \sim 1$ Myr (Pollack et al. 1996; Benz et al.

Hill 半径の中のガスを獲得

$$R_{\rm H} = a\left(\frac{M_{\rm p}}{3M_*}\right)^{1/3},$$

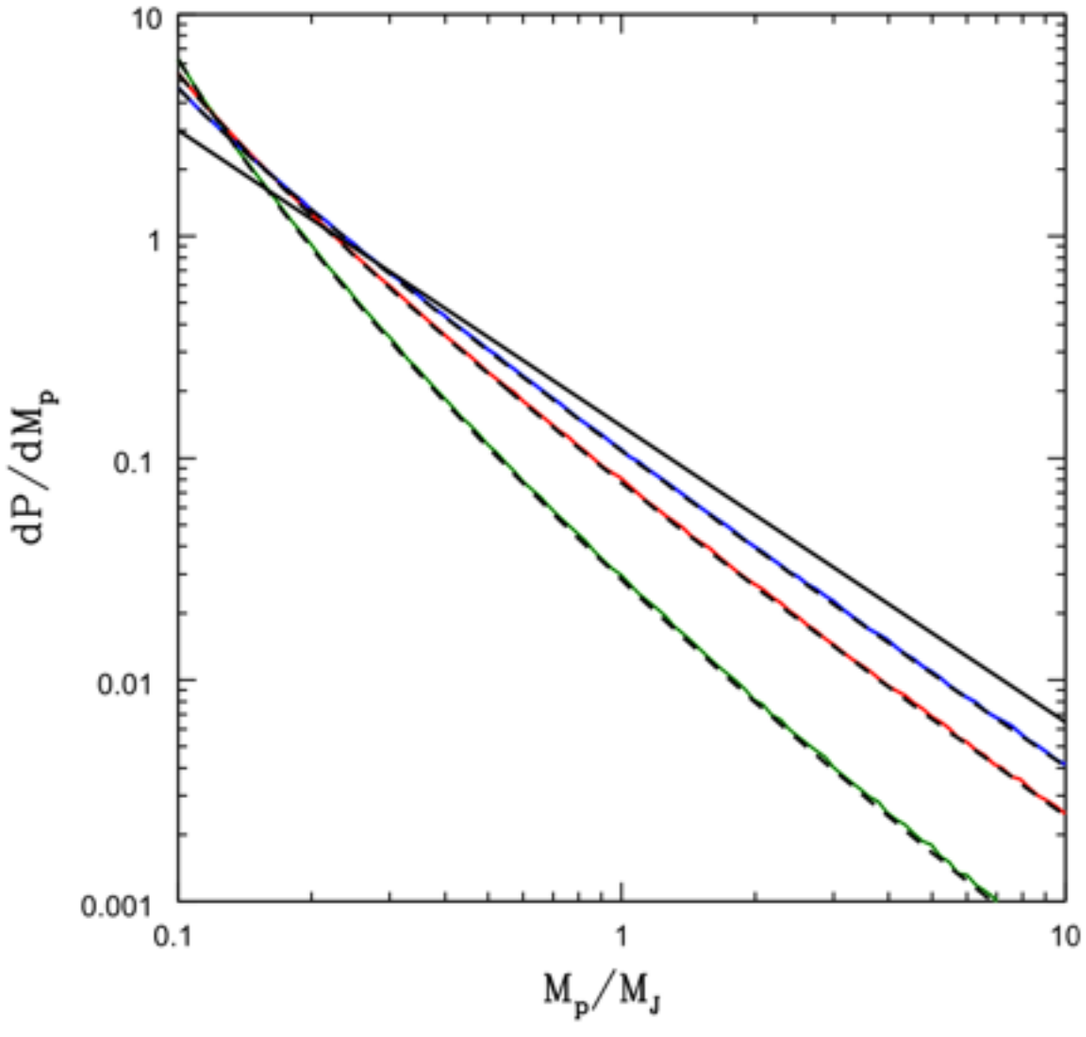

Within current observational uncertainties, disk lifetimes are observed to be exponentially distributed, whereas the PMF has a nearly power-law form. The framework developed in this paper produces a nearly power-law PMF using the exponential distribution of disk lifetimes as input. In order to obtain results consistent with observations, other input parameters—in addition to the disk lifetime—must sample distributions of values, and the mass accretion rate must increase as the planet grows. In the limiting case of a constant mass accretion rate, the exponential distribution of disk lifetimes imprints an exponential falloff in the PMF, which leads to a deficit of larger planets compared to the observed distribution.

他の値がバラつけば良い。

#2 Particle Dynamics in 3D Self-gravitating Disks. I. Spirals, H. Baehr & Z. Zhu, ApJ, 909, 135
#3 Particle Dynamics in 3D Self-gravitating Disks. II. Strong Gas Accretion and Thin Dust Disks, ApJ, 909, 136

局所計算 (shearing box)　PENCIL code

$$\frac{\partial \rho_{\rm g}}{\partial t} - q\Omega x\frac{\partial \rho_{\rm g}}{\partial y} + \nabla\cdot(\rho_{\rm g}\boldsymbol{u}) = f_D(\rho_{\rm g}), \qquad (18)$$

$$\frac{\partial \boldsymbol{u}}{\partial t} - q\Omega x\frac{\partial \boldsymbol{u}}{\partial y} + \boldsymbol{u}\cdot\nabla\boldsymbol{u} = -\frac{\nabla P}{\rho_{\rm g}} + q\Omega v_x\hat{\boldsymbol{y}} - 2\Omega\times\boldsymbol{u} - \nabla\Phi + f_\nu(\boldsymbol{u}),$$

$$\frac{\partial s}{\partial t} - q\Omega x\frac{\partial s}{\partial y} + (\boldsymbol{u}\cdot\nabla)s = \frac{1}{\rho_{\rm g}T}(2\rho_{\rm g}\nu\boldsymbol{S}^2 - \Lambda + f_\chi(s)).$$

$$f(\xi) = \nu(\nabla^6\xi)$$

$$\Lambda = \frac{\rho(c_{\rm s}^2 - c_{\rm s,irr}^2)}{(\gamma-1)t_{\rm c}},$$

$$\Phi(\boldsymbol{k},t) = -\frac{2\pi G\rho(\boldsymbol{k},t)}{\boldsymbol{k}^2},$$

ダストは粒子で扱う

初期の Toomre's Q は 1.02

$$t_c = \beta\Omega^{-1}$$

$$a_{\rm drag} = \frac{|\boldsymbol{w}-\boldsymbol{u}|}{t_s} \sim \frac{c_{\rm s}}{{\rm St}\,\Omega^{-1}}.$$

パラメータによらず pitch 角 〜10° の Spiral が現れる

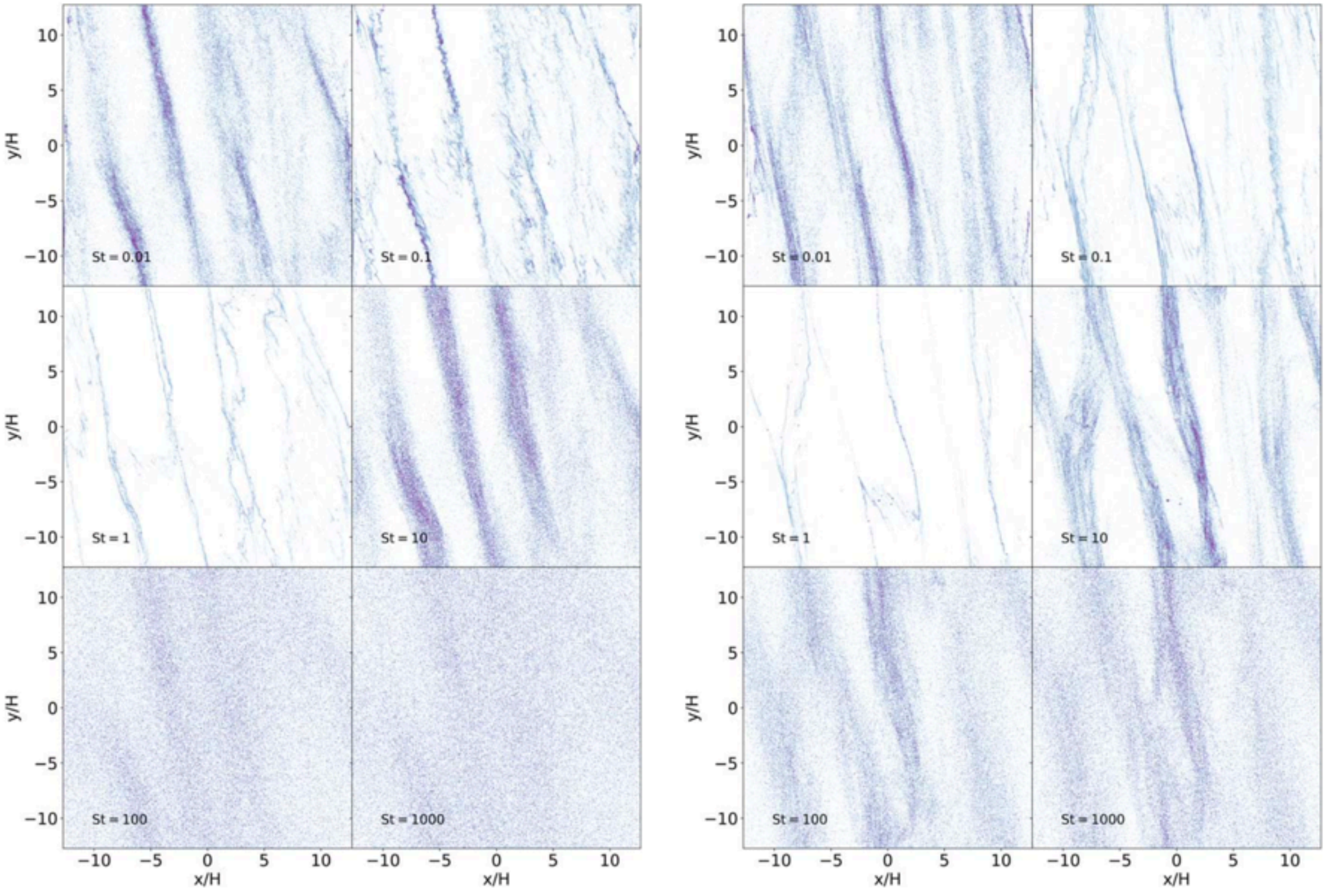

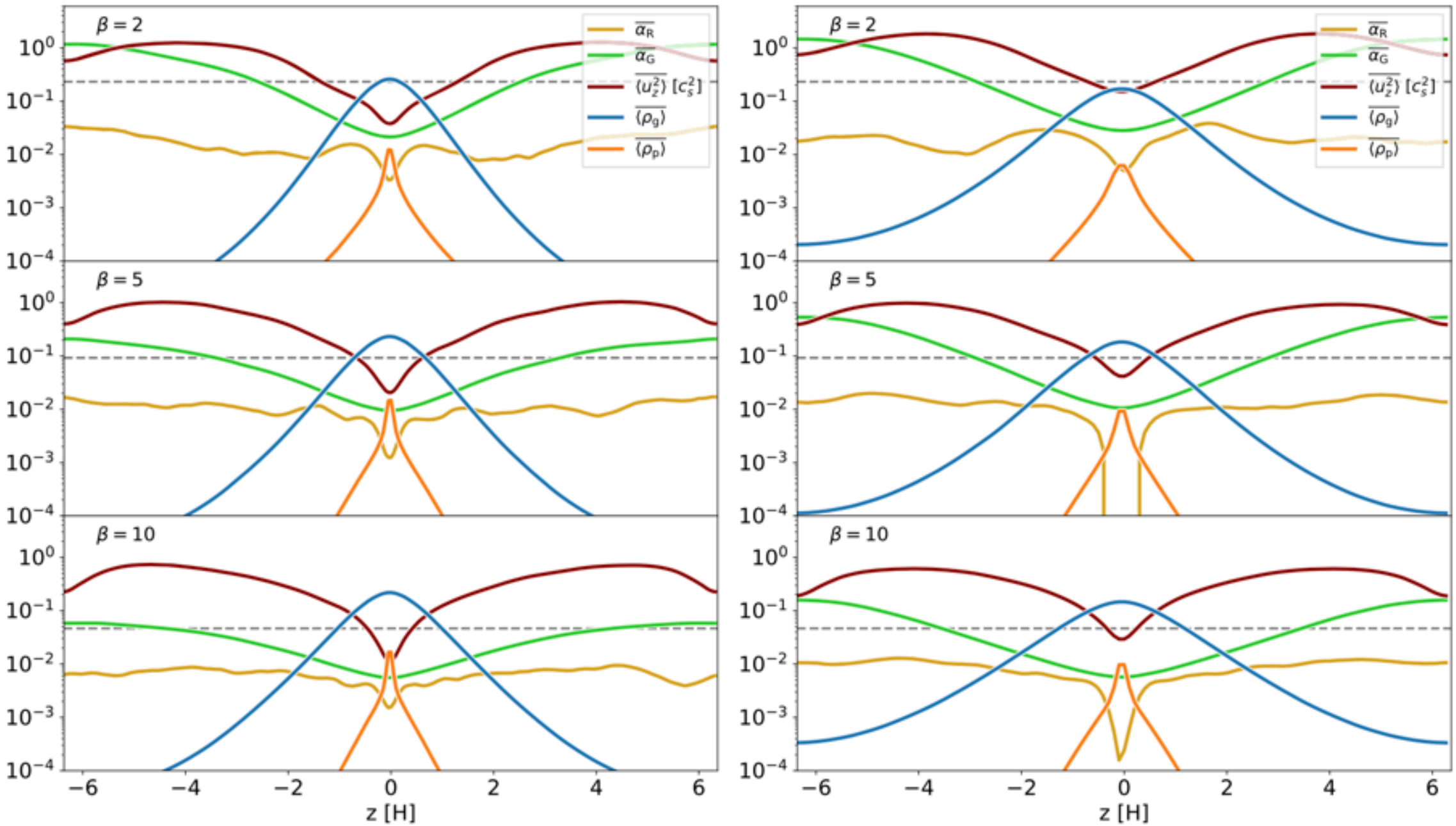
β = 2
β = 5
β = 10
$\overline{\alpha_R}$
$\overline{\alpha_G}$
$\overline{\langle u_z^2\rangle}$ [c_s^2]
$\overline{\langle \rho_g \rangle}$
$\overline{\langle \rho_p \rangle}$
10^0
10^{-1}
10^{-2}
10^{-3}
10^{-4}
−6
−4
−2
0
2
4
6
z [H]

#4 A possible far-ultraviolet flux-dependent core mass function in NGC 6357, J. Brand et al., A&A

450 μm, 850 μm, CO (3-2) (SCUBA-2)

70 μm, 160 μm Hi-GAL Herschel

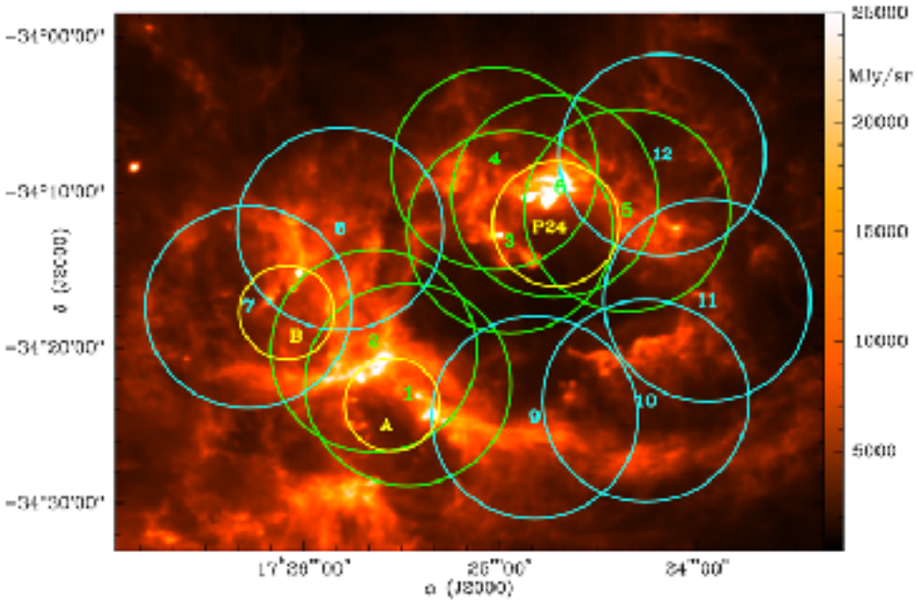

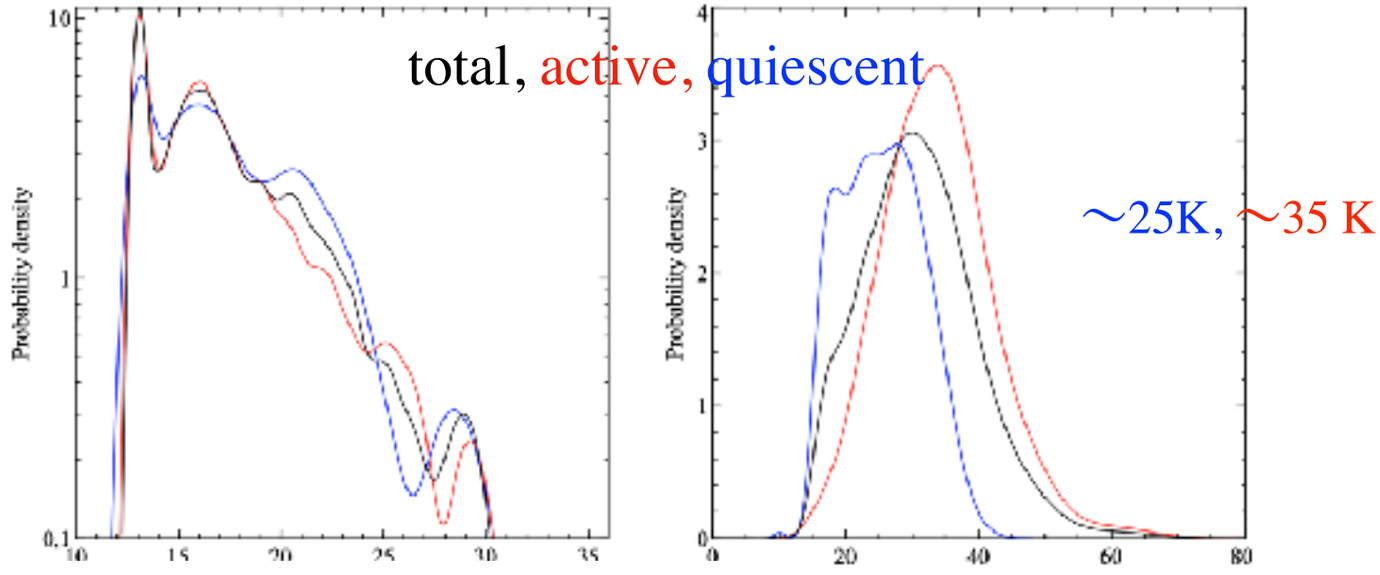

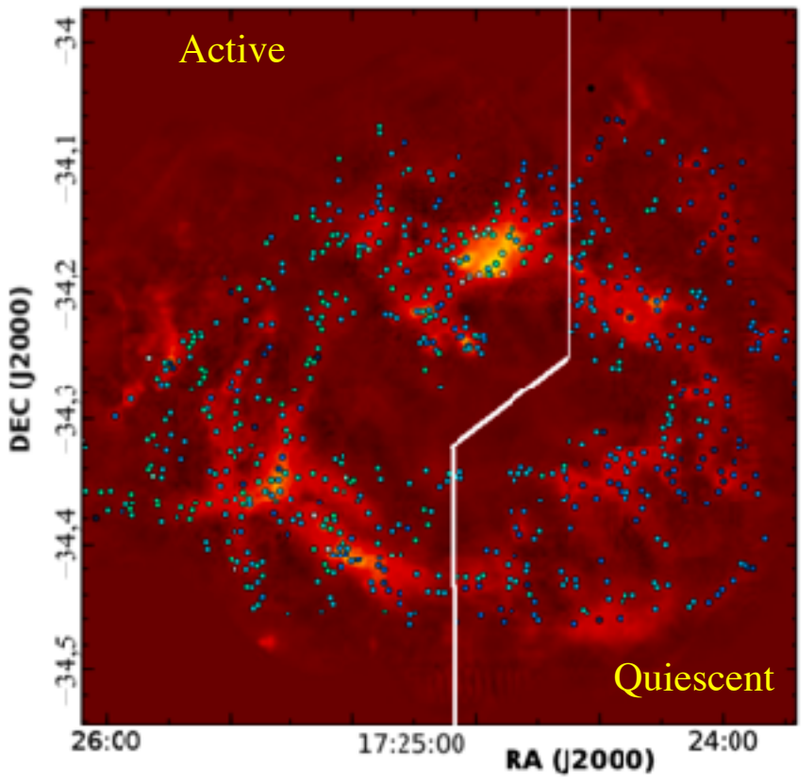

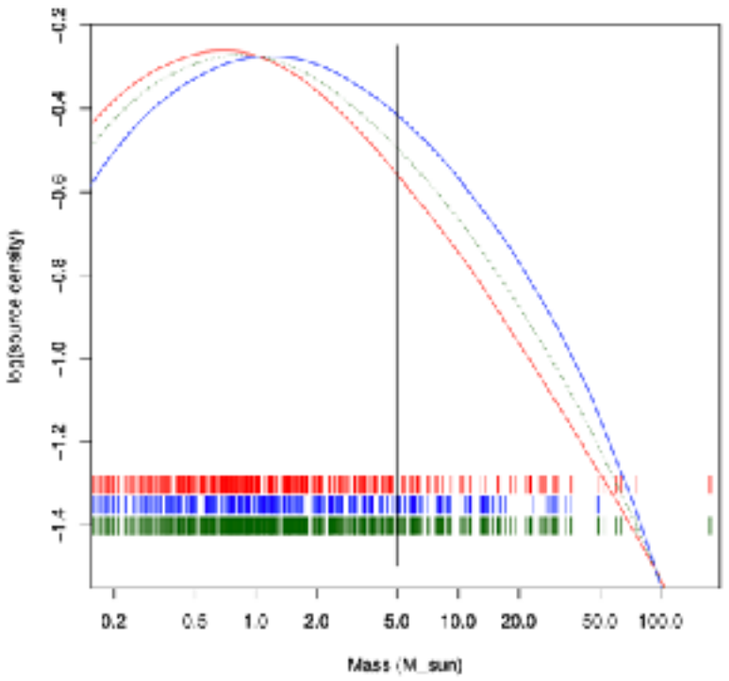

$$M = \gamma D^2 S_\nu / [\kappa_\nu B_\nu(T_{\rm d})],$$

1221 cores のうち686 coreを

SED fit

411 (active), 275 (quiescent)

$d = 1.77 \pm^{0.12}_{0.08}$ kpc

found 51 candidate protostellar and 224 starless cores in the quiescent region, and 160 candidate protostellar and 251 starless cores in the active region. Unfortunately, the sample

3. We derived the core masses by assuming a plausible dust opacity (we also discussed possible effects of FUV radiation). We estimated a mass completeness limit of $\sim 5\,M_\odot$. We found mass-size relations of $\log(M/M_\odot) \sim a \times \log(D/\mathrm{arcsec})$, with a in the range 2.0 – 2.4, consistent with those from other regions or large samples of clumps. The starless cores above the mass completeness limit are likely to be gravitationally bound, hence pre-stellar in nature.
4. The estimated fraction of molecular gas in dense cores is 1.4 % in NGC6357. This is consistent with values from most galactic star formation regions.
5. We showed that the properties of the cores nearer to the HII regions are consistent with pre-existing cores gradually being engulfed in a PDR and photoevaporating.
6. We constructed the CMFs for $M > 5\,M_\odot$, finding a Salpeter-like CMF in the quiescent region ($\alpha \sim 2.1 - 2.4$) and a significantly flatter (at a $2\,\sigma$ level) one in the active region ($\sim 1.7 - 1.9$ with $\alpha = -\mathrm{d}\log(\mathrm{d}N/\mathrm{d}M)/\mathrm{d}\log(M)$). The difference becomes even more significant for pre-stellar cores when using the maximum likelihood estimator ($\alpha \sim 2$ vs. $\alpha \sim 1.2$). We attribute this to the effects of the FUV radiation as well.
7. We compared the CMFs with those predicted by simulations of cloud-cloud collisions, finding no conclusive evidence for cloud-cloud collisions giving rise to the cores, rather than them being pre-existing.

#5 Tracers of the ionization fraction in dense and translucent gas: I. Automated exploitation of massive astrochemical model grids, E. Bron et al. A&A, 645, A28

機械学習　強度比から電離度を推定する最良の輝線ペアを探す

Translucent cloud と Dense cloud の別あり：化学モデル Roueff+15

ρ, T, A_V, 輻射場, 宇宙線, ortho/para, depletion 固定　定常状態

	Translucent medium	Cold dense medium
n_H [cm^{-3}]	3×10^2–3×10^3	10^3–10^6
T_{gas} [K]	15–100	7–20
G_0	1–1000	1
A_V	2–6	5–20
ζ [s^{-1}]	10^{-17}–10^{-15}	10^{-17}–10^{-16}
OPR_{H_2}	0.1–3	10^{-4}–10^{-1}
depletion factor	1	1–10
[S]	1.86×10^{-8}–1.86×10^{-5}	1.86×10^{-8}–1.86×10^{-5}

RF = Random Forest

Translucent

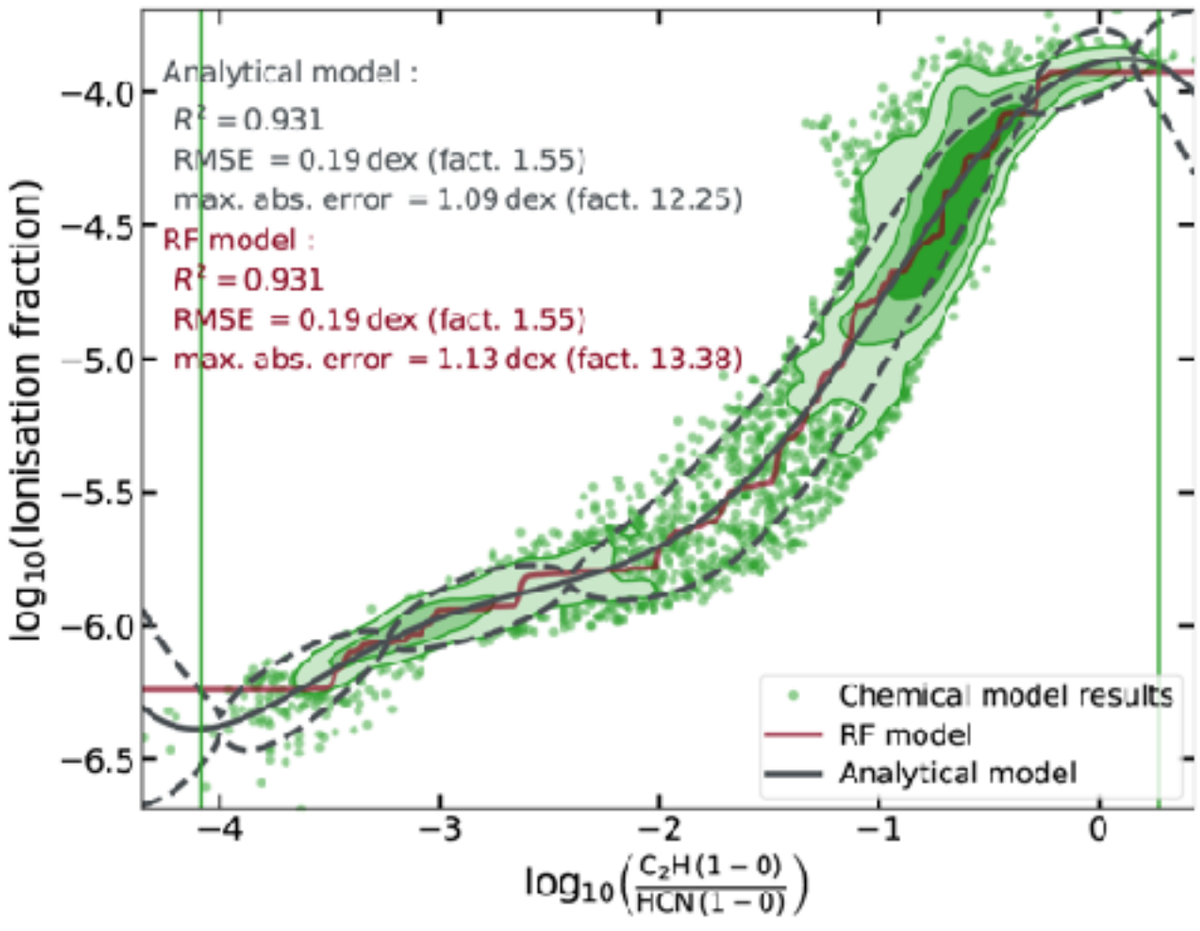

Analytical fit　強度比から電離度を求める近似式

Cold cloud

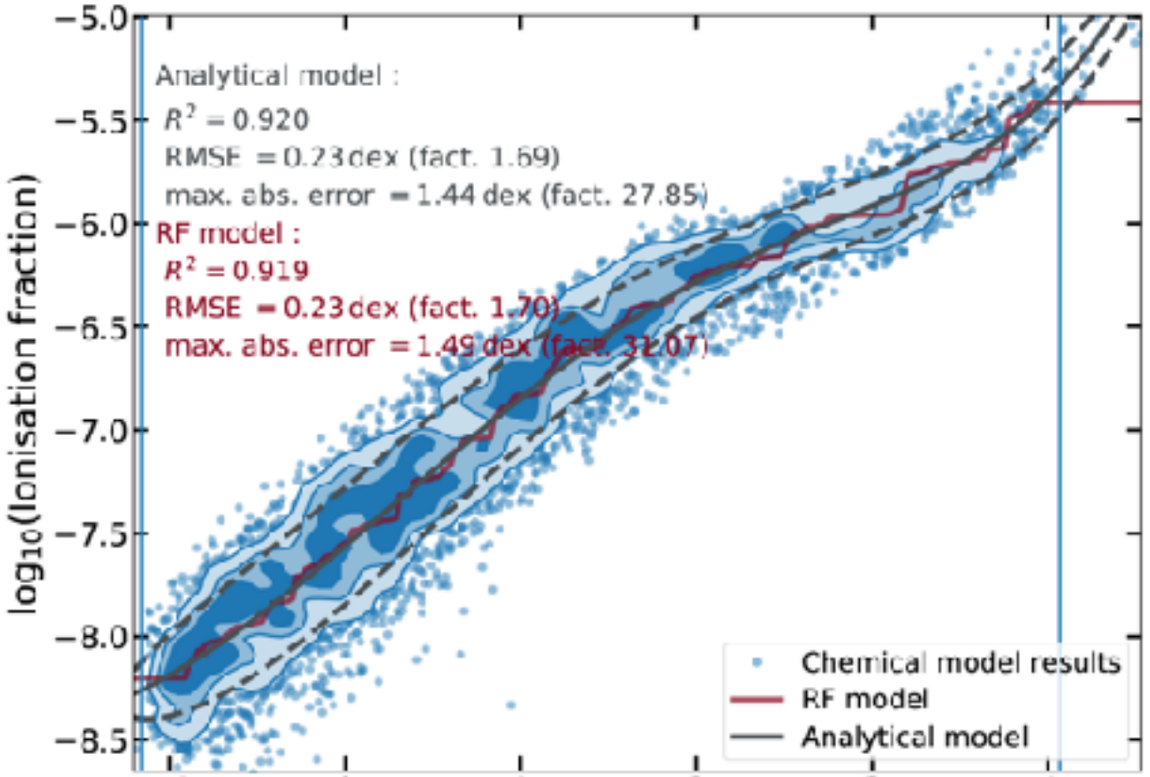

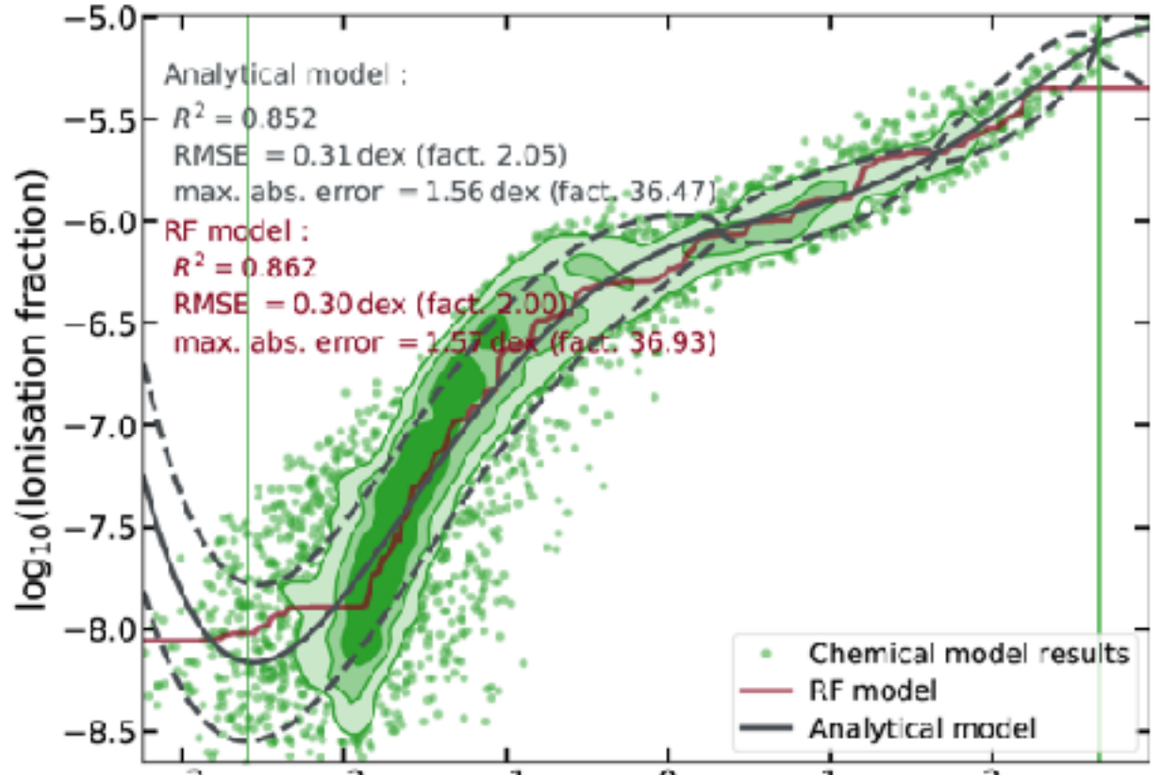

電離率決定精度

$$R^2 = 1 - \frac{SS_{\text{res}}}{SS_{\text{tot}}} \quad \text{with the sums of squares}$$

$$SS_{\text{res}} = \sum_i \left(y_i^{\text{pred}} - y_i^{\text{true}}\right)^2 \quad \text{and} \quad SS_{\text{tot}} = \sum_i \left(\overline{y^{\text{true}}} - y_i^{\text{true}}\right)^2,$$

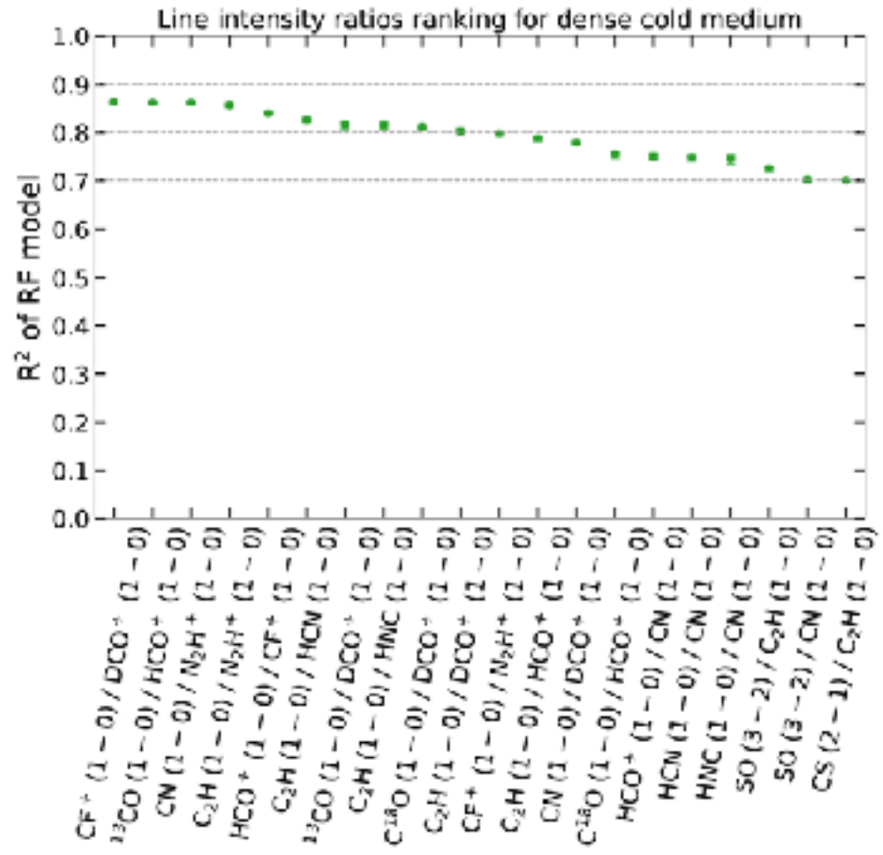

著者たちのお勧め

- In translucent medium conditions, we recommend the use C_2H (1–0)/HCN (1–0), C_2H (1–0)/HNC (1–0), or C_2H (1–0)/CN (1–0). If sensitivity is an issue, HCN (1–0)/CF^+ (1–0) can sometimes perform as well as the previously listed ratios.

- In cold dense gas conditions, we recommend the use of CF^+ (1–0)/DCO^+ (1–0), ^{13}CO (1–0)/HCO^+ (1–0) or CN (1–0)/N_2H^+ (1–0) if detectability is not an issue for these species, and of ^{13}CO (1–0)/HCO^+ (1–0) or $C^{18}O$ (1–0)/ HCO^+ (1–0) otherwise.

However, our results show that even in the cold dense gas regime, and despite including DCO^+ in our list of potential tracers, the DCO^+/HCO^+ column density ratio is not ranked among the best tracers of the ionization fraction. In fact, it is ranked as the 38^{th} best tracer in dense cold gas conditions, with a R^2 of 0.57 only(cf. Table B.7).

#6 Radial Velocity Monitoring of the Young Star Hubble 4: Disentangling Starspot Lifetimes from Orbital Motion, A. Carvalho et al. ApJ?

Hubble 4　K7 型 1.234 Mo + 0.73 Mo 連星 4.1 au

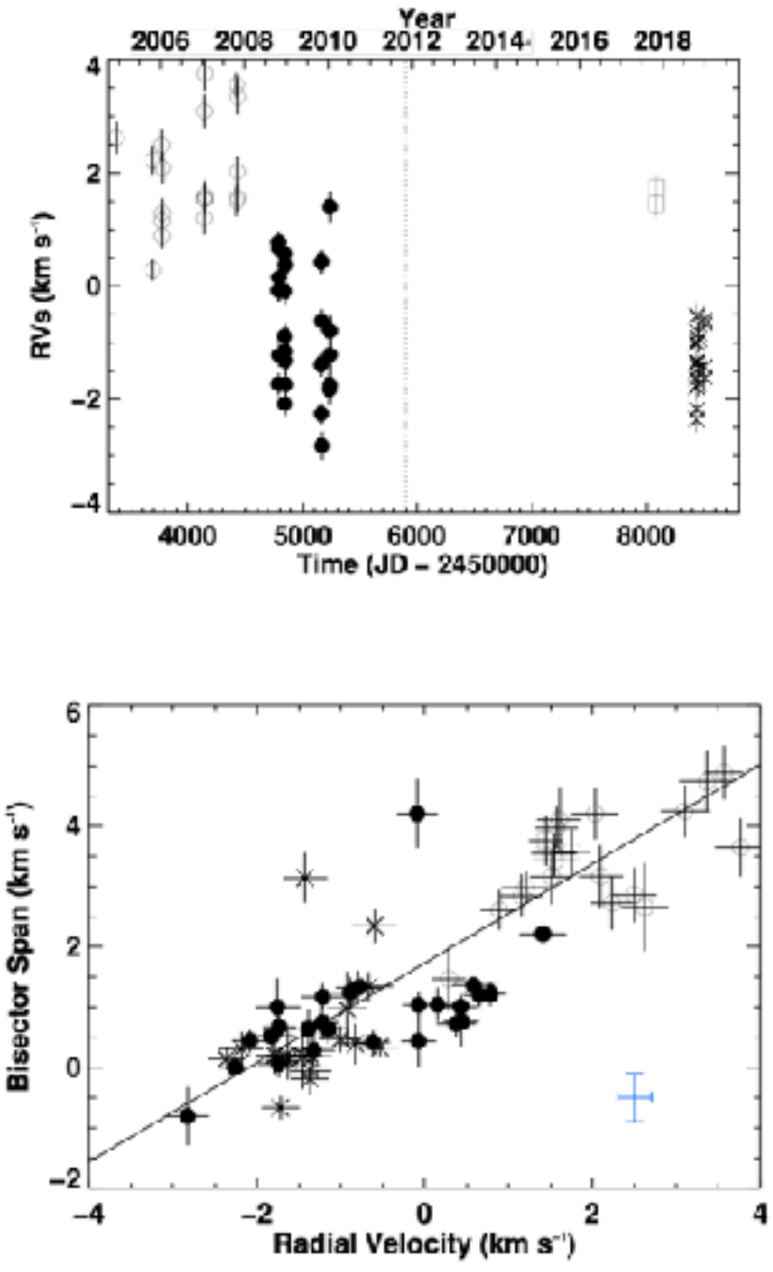

Line Center (RV) と CCF に相関

RVの変動は 公転＋磁場

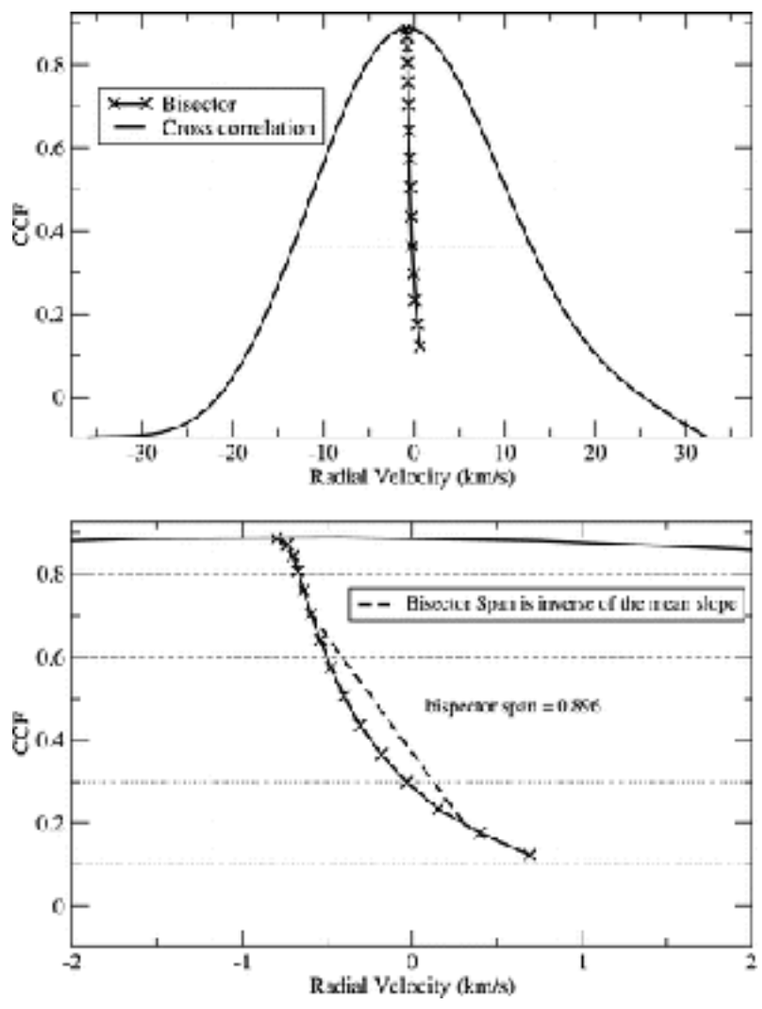

Huerta+08 Bisector の説明

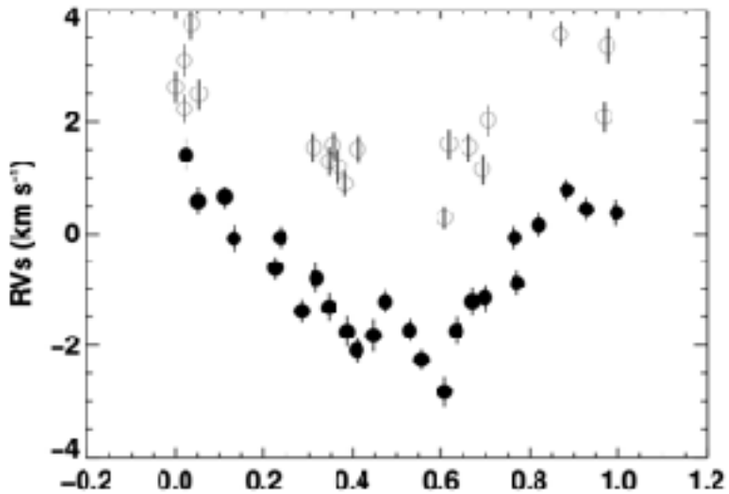

1.5459日周期の変動

○2005-2007　●2008-2010

公転ではない変動が持続

#7 The Extraordinary Outburst in the Massive Protostellar System NGC 6334 I-MM1: Spatiokinematics of Water Masers during a Contemporaneous Flare Event, ApJ, 908, 175

MM1: 2008-2015に70±20倍増光

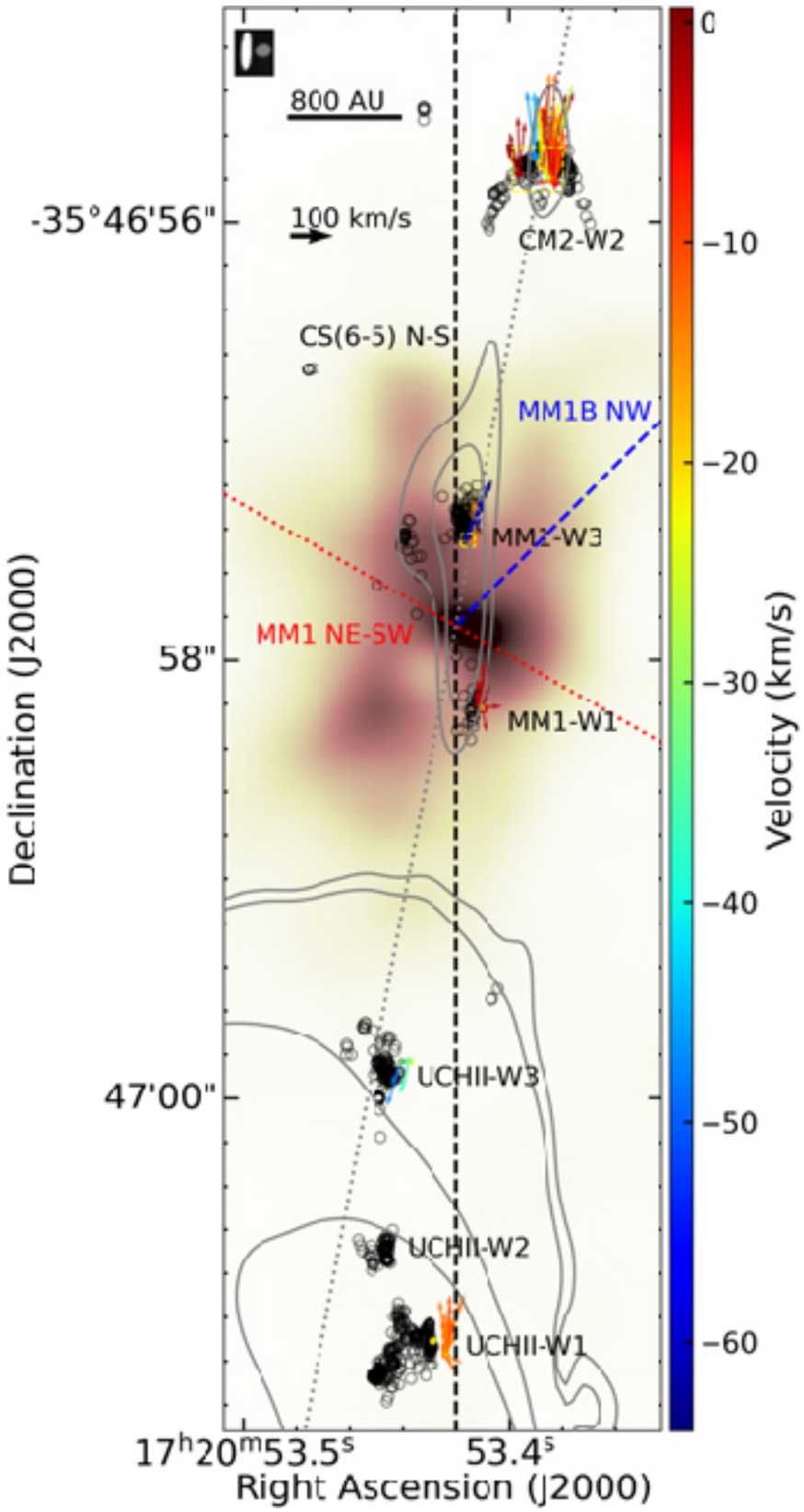

$d = 1.30 \pm 0.09$ kpc

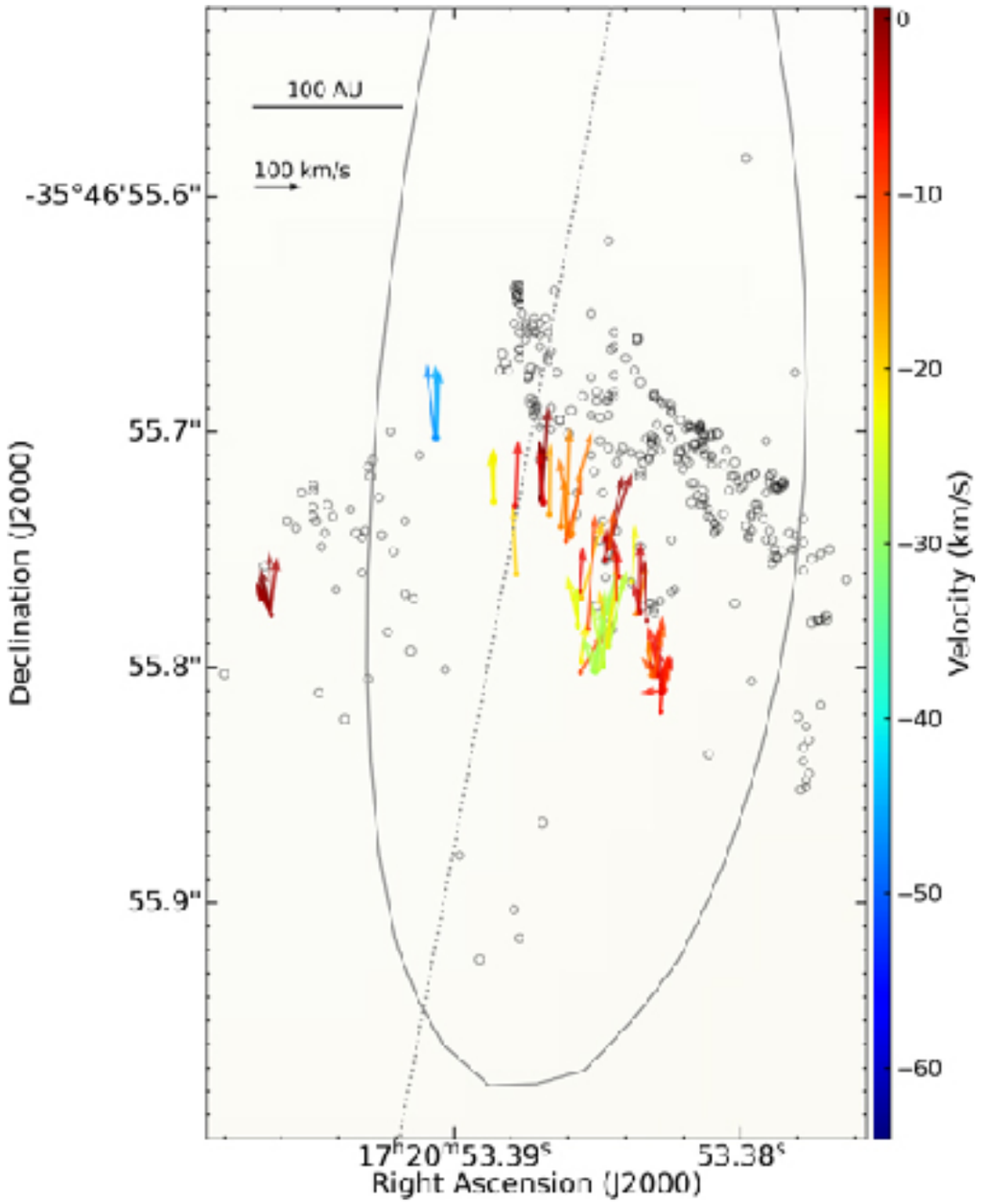

固有運動